Biotechnol Lett

Microbial and Enzyme Technology

Stabilization of human immunodeficiency virus type 1 reverse transcriptase by site-directed mutagenesis

Kosaku Nishimura, Mayu Shinomura, Atsushi Konishi, Kiyoshi Yasukawa*

Division of Food Science and Biotechnology, Graduate School of Agriculture,
Kyoto University, Sakyo-ku, Kyoto 606-8502, Japan

Abbreviations: AMV, avian myeloblastosis virus; DMSO, dimethyl sulfoxide; HIV-1, human immunodeficiency virus type 1; HIV-1 M, HIV-1 group M; HIV-1 O, HIV-1 group O; MMLV, Moloney murine leukemia virus; PMSF, phenylmethylsulfonyl fluoride; RT, reverse transcriptase; T/P, template-primer; TCA, trichloroacetic acid.

*Corresponding author. Tel: +81-75-753-6267, Fax: +81-75-753-6265, E-mail address: yasukawa@kais.kyoto-u.ac.jp

Key words: human immunodeficiency virus type 1; reverse transcriptase; site-directed mutagenesis; thermostability.

Human immunodeficiency virus type 1 (HIV-1) reverse transcriptase (RT) is a heterodimer containing 66-kDa p66 and 51-kDa p51 subunits. We previously showed that HIV-1 group M (HIV-1 M) RT and HIV-1 group O (HIV-1 O) RT have higher affinities for dTTP and template-primer (T/P) than Moloney murine leukemia virus (MMLV) RT, which is currently used for cDNA synthesis, suggesting that they might also be useful for cDNA synthesis (Konishi et al. (2013) Appl Biochem Biotechnol 169:77−87). In this study, we increased the thermostability of both HIV-1 M RT and HIV-1 O RT by site-directed mutagenesis. The Asp443→Ala mutation, which is known to abolish RNase H activity, was introduced into the p66 subunits of HIV-1 M RT and HIV-1 O RT. The temperatures that reduced the initial activity by 50% in a 10 min incubation (T_{50}) of the resulting mutants, HIV-1 M $p66_{D443A}$/p51 and HIV-1 O $p66_{D443A}$/p51, were 44°C and 52°C, respectively, which were higher than those of wild-type HIV-1 M p66/p51 (42°C) and HIV-1 O p66/p51 (48°C), respectively. The highest temperature at which both HIV-1 M $p66_{D443A}$/p51 and HIV-1 O $p66_{D443A}$/p51 exhibited cDNA synthesis activity was 68°C, a higher temperature than for the wild-type enzymes (62°C and 66°C, respectively).

Introduction

Reverse transcriptase (RT) is the enzyme responsible for viral genome replication. Human immunodeficiency virus type 1 (HIV-1) RT is a heterodimer consisting of a 66-kDa p66 subunit and a 51-kDa p51 subunit. The p66 subunit comprises the fingers, palm, thumb, and connection subdomains and the RNase H domain, and the p51 subunit is composed of the fingers, palm, thumb, and connection subdomains, but is lacking in the RNase H domain (di Marzo Veronese et al. 1986; Patel et al. 1995; Ding et al. 1998). HIV-1 RT is widely used as a tool in the development of inhibitors for the treatment of HIV-1 infection. It is not used for cDNA synthesis due to its low fidelity. Moloney murine leukemia virus (MMLV) RT and avian myeloblastosis virus (AMV) RT are widely used for cDNA synthesis due to their high fidelity (Kimmel and Berger, 1987).

HIV-1 is classified into four phylogenetic major groups: M (main), O (outlier), N (non-M/non-O), and P. HIV-1 group M (HIV-1 M) infection is spread all over the world, whereas HIV-1 group O (HIV-1 O) infection is restricted to Cameroon and neighboring countries in West Central Africa (Buonaguro et al. 2007). The amino-acid sequence homology between HIV-1 M RT and HIV-1 O RT is 79% (Quiňones-Mateu et al. 1997; Buonaguro et al. 2007). We previously showed that for the incorporation of dTTP into poly(rA)-p$(dT)_{15}$, HIV-1 M RT and HIV-1 O RT have higher affinities for dTTP and template-primer (T/P) than MMLV RT, and are less susceptible to formamide, which is frequently used for cDNA synthesis of a G+C-rich RNA than MMLV RT. Indeed, in RT-PCR, low fidelity of RT is problematic for the cloning of cDNA. However, high fidelity is not often required for the detection of target RNA molecules. Hence, the use of HIV-1 RT for cDNA synthesis might be attractive for the detection of certain target

RNA molecules (Konishi et al. 2013).

HIV-1 RT exists not only as a p66/p51 heterodimer, but also as a p66-subunit homodimer, $(p66)_2$, or a p51-subunit homodimer, $(p51)_2$. In HIV-1 M RT, based on the fact that monomeric p51 and p66 are inactive, the dissociation constants (K_d) of p51 and p66, p66 and p66, and p51 and p51 were determined to be 0.31, 4.2, and 230 μM, respectively (Venezia et al. 2006). It was recently reported that the K_d values of p66/p51, $(p66)_2$, and $(p51)_2$ for template-primer (T/P) are 3.9, 9.8, and 440 nM, respectively (Marko et al. 2013).

For cDNA synthesis, a higher reaction temperature is desirable because it reduces RNA secondary structures and nonspecific primer binding. Therefore, improving the thermal stability of RT is an important aim. The thermostabilities of MMLV RT and AMV RT have been improved by eliminating the RNase H activity (Kotewicz et al. 1998; Gerard et al. 2002; Mizuno et al. 2010), by introducing positive charges at positions that have been implicated in the interaction with T/P (Yasukawa et al. 2010b; Konishi et al. 2012), and by random mutagenesis (Arezi and Hogrefe, 2009; Baranauskas et al. 2012). This study aimed to increase the thermostabilities of HIV-1 M RT and HIV-1 O RT. We introduced the Asp443→Ala mutation, which abolishes the RNase H activity, into the p66 subunit of both RTs. Our results indicate that the mutant RTs have higher stability than the wild-type p66/p51 enzymes.

Materials and methods

Materials

p(dT)$_{15}$ was purchased from Life Technologies Japan Ltd. (Tokyo, Japan). [methyl-^{3}H]dTTP (1.52 TBq/mmol) and poly(rA) were from GE Healthcare (Buckinghamshire, UK). The RT concentration was determined by the method of Bradford (Bradford, 1976) using Protein Assay CBB Solution (Nacalai Tesque, Kyoto, Japan) with bovine serum albumin (Nacalai Tesque) as standard. Standard RNA, an RNA of 1014-nucleotides corresponding to DNA sequence 8353–9366 of the *cesA* gene of *Bacillus cereus* (GenBank accession no. DQ360825), was prepared by an *in vitro* transcription (Yasukawa et al. 2010a).

Bacterial strains, plasmids and transformation

pET-HisHIVMp51, pET-HisHIVMp66, pET-HisHIVOp51, and pET-HisHIVOp66 are expression plasmids for N-terminally (His)$_6$-tagged HIV-1 M p51, HIV-1 M p66, HIV-1 O p51, and HIV-1 O p66, respectively (Fig. 1). To introduce the mutation of Asp443→Ala in the p66 subunit, Quikchange method was carried out with the plsamid pET-HIVMp66 and the primers pHIVMD443A 5’-GCAGAAACTTTTTATGTGGCCGGAGCTGCG-3’ (mismatch is underlined) and pHIVMD443A_CP 5’-CGCAGCTCCGGCCACATAAAAGTTTCTGC-3’ for HIV-1 M RT and the plasmid pET-HIVOp66 and the primers pHIVOD443A 5’-GCTGAAACCTTCTACGTCGCTGGTGCGGCC-3’ and pHIVOD443A_CP 5’-GCCGCACCAGCGACGTAGAAGGTTTCAGC-3’ for HIV-1 O RT. The resulted plsamids were named pET-HIVMp66$_{D443A}$ and pET-HIVOp66$_{D443A}$, respectively. *E. coli* BL21(DE3) [F^{-}, *ompT*, *hsdS*$_B$(r_B^{-} m_B^{-}) *gal dcm* (DE3)] cells were transformed with each plasmid and cultured in L broth. Ampicillin was used at the concentration of 50 μg/ml.

Fig. 1

Expression and purification of HIV-1 M RT and HIV-1 O RT

The overnight culture of the transformants (20 mL) was added to 2,000 mL of L broth in a 2-liter flask and incubated with vigorous aeration by air-pump at 37ºC. When OD_{660} reached 0.6–0.8, 0.8 mL of 0.5 M IPTG was added and growth was continued at 30ºC for 4 h. After centrifugation at 10,000 × *g* for 10 min, the cells were harvested, suspended with 20 mL of 0.02 M potassium phosphate, 2.0 mM dithiothreitol (DTT), 10% glycerol, pH 7.2 (buffer A) containing 1 mM phenylmethylsulfonyl fluoride (PMSF). For the production of $(p51)_2$ and $(p66)_2$, the suspension containing the N-terminally $(His)_6$-tagged p51 and that containing the N-terminally $(His)_6$-tagged p66 were used, respectively. For the production of p66/p51, the mixture of the above suspensions was used. They were disrupted by sonication. After centrifugation at 15,000 × *g* for 20 min, the supernatant was collected and applied to a column [25 mm (inner diameter) × 120 mm] packed with Toyopearl DEAE-650M gel (Tosoh, Tokyo, Japan) equilibrated with buffer A. The pass-through was collected, to which solid $(NH_4)_2SO_4$ was added to a final concentration of 40% saturation. After centrifugation at 20,000 × *g* for 20 min, the pellet was collected and dissolved in 10 mL of 50 mM Tris-HCl, 200 mM KCl, 2.0 mM DTT, 10% glycerol, pH 8.3 (buffer B) and applied to the column packed with a Ni^{2+}-sepharose (HisTrap HP 1 mL, GE Healthcare, Buckinghamshire, UK) equilibrated with buffer B containing 50 mM imidazole. The bound RT was eluted with buffer B containing 500 mM imidazole. The eluate was dialyzed against 50 mM Tris-HCl, 200 mM KCl, 50% glycerol, pH 8.3, and stored at −80°C.

Sodium dodecyl sulfate-polyacrylamide gel electrophoresis (SDS-PAGE)

SDS-PAGE was performed in a 10% polyacrylamide gel under reducing conditions. Proteins were reduced by treatment with 2.5% (v/v) of 2-mercaptoethanol at 100ºC for 10 min, and then applied onto the gel. A constant current of 40 mA was applied for 40 min. After electrophoresis, proteins were stained with Coomassie Brilliant Blue R-250. The molecular mass marker kit consisting of rabbit muscle phosphorylase B (97.2 kDa), bovine serum albumin (66.4 kDa), hen egg white ovalbumin (44.3 kDa), and bovine carbonic anhydrase (29.0 kDa) was purchased from Takara Bio Inc (Otsu, Japan).

Measurement of RT activity for incorporation of dTTP into poly(rA)-p$(dT)_{15}$

RT activity for incorporation of dTTP into poly(rA)-p$(dT)_{15}$ was measured as described previously (Yasukawa et al. 2008; 2009). Briefly, the reaction was carried out in 25 mM Tris-HCl (pH 8.3), 50 mM KCl, 2.0 mM DTT, 5.0 mM $MgCl_2$, 25 µM poly(rA)-p$(dT)_{15}$ (this concentration is expressed as that of p$(dT)_{15}$), 0.2 mM [^{3}H]dTTP, and active fractions or purified preparations of RT at 37ºC. An aliquot (20 µL) was taken from the reaction mixture at a predetermined time and immediately spotted onto the glass filter GF/C 2.5 cm (Whatman, Middlesex, UK). The amounts of [^{3}H]dTTP incorporated was counted, and the initial reaction rate was determined.

Measurement of RT activity for cDNA synthesis

RT activity for cDNA synthesis was measured as described previously (Yasukawa et al. 2010a). Briefly, the reaction (20 µL) was carried out in 25 mM Tris-HCl (pH 8.3), 50 mM KCl, 2.0 mM DTT, 0.1 mM dNTP, 0.5 µM primer RV-R26 5'-TGTGGAATTGTGAGCGGTGTCGCAATCACCGTAACACGACGTAG-3', 0.8 pg/µL (corresponding to 2 pM) standard RNA, and various concentrations (0–100 nM) of RT at 46ºC for 30 min and stopped by heating at 95ºC for 5 min. The PCR reaction (30 µL) was then carried out in 50 mM KCl, 10 mM Tris-HCl (pH 8.3), 1.5 mM $MgCl_2$, 0.5 µM (each) primers F5 5'-TGCGCGCAAAATGGGTATCAC-3' and RV 5'-TGTGGAATTGTGAGCGG-3', 0.1 mM dNTP, 10% v/v product of the reverse transcriptase reaction, and 0.05 U/µl Taq polymerase. The cycling parameters were 95ºC for 30 s, followed by 30 cycles at 95ºC for 30 s, 55ºC for 30 s, and 72ºC for 60 s. The amplified products were separated on 1.0% agarose gels and stained with ethidium bromide (1 µg/mL).

Results

Comparison of activities of $(p51)_2$, $(p66)_2$ and p66/p51 from HIV-1 M and HIV-1 O

It has been reported that for HIV-1 M RT, $(p51)_2$ is less active than $(p66)_2$ and p66/51 (Le Grice et al. 1991; Hostomsky et al. 1992; Bavand et al. 1993). However, such comparison was not reported for HIV-1 O RT. Hence, we prepared $(p51)_2$, $(p66)_2$, and p66/51 from HIV-1 M and HIV-1 O and evaluated their activities. Figure 1 shows the expression plasmids for p66 and p51 of HIV-1 M and HIV-1 O, whereas each contained N-terminal $(His)_6$. BL21(DE3) cells were transformed with each plasmid. Purification

of $(p51)_2$ and $(p66)_2$ was carried out from the cells expressing p51 or p66, respectively, and purification of p66/p51 was carried out from a mixture of these cells. By SDS-PAGE analysis of the purified RT preparations of HIV-1 M and HIV-1 O, $(p51)_2$ yielded a single band with a molecular mass of 51 kDa, $(p66)_2$ yielded a single band with a molecular mass of 66 kDa, and p66/p51 yielded two bands with molecular masses of 51 and 66 kDa (Fig. 2).

Fig. 2

Figure 3 shows the results of steady-state kinetic analysis of RT in the incorporation of dTTP into poly(rA)-p$(dT)_{15}$ (T/P). The dependences of the initial reaction rate (v_o) on dTTP (Fig. 3A, C) and T/P (Fig. 3B, D) concentrations exhibited the Michaelis–Menten curves. The $K_{m,dTTP}$, $K_{m,T/P}$, and k_{cat} values were determined (Table 1). In HIV-1 M and HIV-1 O, the $K_{m,dTTP}$ and $K_{m,T/P}$ values of $(p51)_2$ were both higher than those of p66/p51, whereas those of $(p66)_2$ and p66/p51 were similar. The k_{cat} values of $(p51)_2$ and $(p66)_2$ were lower than those of p66/p51 were. The $K_{m,dTTP}$ and k_{cat} values of $(p51)_2$, $(p66)_2$ and p66/p51 of HIV-1 M were lower than those of $(p51)_2$, $(p66)_2$ and p66/p51 of HIV-1 O, respectively. This indicates that HIV-1 M RT has higher affinity for dTTP, but lower processivity than HIV-1 O RT.

Fig. 3

Table 1

The cDNA synthesis activities of RT are shown in Fig. 4. The reaction was carried out at 46°C for 30 min with varying enzyme concentrations from 0–100 nM, followed by PCR of the cDNA synthesis reaction products and agarose gel electrophoresis of the PCR products. For the cDNA synthesis using $(p51)_2$ of HIV-1 M and HIV-1 O, PCR-amplified products with the expected size of 601 bp were not detected. For the cDNA synthesis with $(p66)_2$ of HIV-1 M and HIV-1 O, the PCR-amplified products were detected for RT concentrations from 1×10^{-4}–10 nM, but not for 1×10^{-6}, 1×10^{-5}, or 100 nM. For the cDNA synthesis with p66/p51 of HIV-1 M and HIV-1 O, the

Fig. 4

PCR-amplified product was detected for RT concentrations from 1×10^{-5}–10 nM, but not 1×10^{-6} or 100 nM. The band densities of the PCR-amplified products from the cDNA synthesis reaction products with $(p66)_2$ were lower than those from the cDNA synthesis reaction products with p66/p51 for RT concentrations of 1×10^{-5} – 1×10^{-3} nM. This indicates that in cDNA synthesis, $(p51)_2$ lacks activity, $(p66)_2$ has low activity, and p66/p51 has high activity. It also indicates that there is no difference in activity between HIV-1 M RT and HIV-1 O RT.

Stabilization of HIV-1 M p66/p51and HIV-1 O p66/p51 by the Asp443→Ala mutation

We previously introduced the Asp524→Ala mutation into MMLV RT and the Asp450 →Ala mutation into AMV RT and generated RT variants without RNase H activity and with increased thermostability (Yasukawa et al. 2010; Konishi et al. 2012). Based on a sequence comparison of MMLV RT, AMV RT, HIV-1 M RT, and HIV-1 O RT, Asp524 of MMLV RT and Asp450 of AMV RT were found to correspond to Asp443 of HIV-1 M RT and HIV-1 O RT. Therefore, we introduced the Asp443→Ala mutation in the p66 subunits of HIV-1 M RT and HIV-1 O RT. The variant enzymes, named HIV-1 M $p66_{D443A}$/p51 and HIV-1 O $p66_{D443A}$/p51, were purified. By SDS-PAGE under reducing conditions, HIV-1 M $p66_{D443A}$/p51 and HIV-1 O $p66_{D443A}$/p51 yielded two bands with molecular masses of 51 and 66 kDa (data not shown). By defining one unit of RT as the amount that incorporates 1 nmol of dTTP into poly(rA)-$p(dT)_{15}$ in 10 min at 37°C, the specific activities of HIV-1 M $p66_{D443A}$/p51 and HIV-1 O $p66_{D443A}$/p51 were 1,400 and 3,500 units/mg, respectively. These activities were almost the same as

those of the wild-type enzymes, as HIV-1 M p66/p51 and HIV-1 O p66/p51 had activities of 1,900 and 5,000 units/mg, respectively (Konishi et al. 2013).

The remaining activities of RT, allowing incorporation of dTTP into T/P after thermal treatment at 42–56 °C for 10 min, are shown in Fig. 5. The relative activities, which were defined as the ratio of the initial reaction rate with incubation at the indicated temperature for 10 min to that without incubation, of all RTs decreased with increasing temperature. In HIV-1 M and HIV-1 O, the relative activities of $(p51)_2$ were lower than those of $(p66)_2$ and p66/p51 were at all temperatures examined. The temperatures that reduced the initial activity by 50% in a 10-min incubation (T_{50}) of HIV-1 M $(p51)_2$, $(p66)_2$, p66/p51, and $p66_{D443A}$/p51 were 42°C, 42°C, 42°C, and 44°C, respectively, and those of HIV-1 O $(p51)_2$, $(p66)_2$, p66/p51, and $p66_{D443A}$/p51 were less than 42°C, 44°C, 48°C, and 52°C, respectively. The finding that for HIV-1 M and HIV-1 O, the T_{50} of $p66_{D443A}$/p51 was higher than for p66/p51 indicates that the Asp443→Ala mutation increases the thermostability of HIV-1 M p66/p51 and HIV-1 O p66/p51, similar to the Asp524→Ala in MMLV RT (Yasukawa et al. 2010b) and the Asp450→Ala in AMV RT mutations (Konishi et al. 2012). The result that the T_{50} of HIV-1 O p66/p51 was higher than that of HIV-1 M p66/p51 and that the T_{50} of HIV-1 O $p66_{D443A}$/p51 was higher than that of HIV-1 M $p66_{D443A}$/p51 indicates that HIV-1 O RT is more stable than HIV-1 M RT, in agreement with a previous report (Menéndez-Arias et al. 2001; Álvarez et al. 2009).

Fig. 5

The dependence on reaction temperature of HIV-1 RT-catalyzed cDNA synthesis is shown in Fig. 6. We carried out cDNA synthesis with 1 nM RT. The highest temperatures at which cDNA synthesis occurred using HIV-1 M $p66_{D443A}$/p51 was

Fig. 6

68°C, higher than that of HIV-1 M p66/p51 (62°C), and the temperature using HIV-1 O $p66_{D443A}$/p51 was 68°C, higher than that of HIV-1 O p66/p51 (66°C). This indicates that the Asp443→Ala mutation in the p66 subunits increases the thermostabilities of HIV-1 M p66/p51 and HIV-1 O p66/p51.

Discussion

In this study, the Asp443→Ala mutation increased T_{50} by 2ºC (from 42ºC to 44ºC) for HIV-1 M p66/p51 and by 4ºC (from 48ºC to 52ºC) for HIV-1 O p66/p51. It also increased the highest temperature at which the cDNA synthesis reaction occurred by 6ºC (from 62 to 68ºC) for HIV-1 M p66/p51 and by 2ºC (from 66 to 68ºC) for HIV-1 O p66/p51. In a previous study of MMLV RT, the Asp524→Ala mutation increased the T_{50} by 3ºC (from 45ºC to 48ºC) and increased the highest temperature at which the cDNA synthesis reaction occurred by 2ºC (from 54 to 56ºC) (Yasukawa et al. 2010b). For HIV-1 M RT, HIV-1 O RT, and MMLV RT, the degree of stabilization conferred by a mutation that abolishes RNase H activity is similar.

Previously, we showed that the theromostabilities of MMLV RT (Yasukawa et al. 2010b) and AMV RT (Konishi et al. 2012) could be increased by introducing positive charges at positions that had been implicated in the interaction with T/P. The mutations introduced were Glu286→Arg, Glu302→Lys, and Leu435→Arg in MMLV RT and Val238→Arg and Leu388→Arg in AMV RT. Sequence comparison showed that Glu286, Glu302, and Leu435 of MMLV RT correspond to Val238, Lys254, and Leu388, respectively, of AMV RT, and Pro243, Lys259, and Lys390, respectively of both HIV-1 M RT and HIV-1 O RT. Based on this data, we prepared HIV-1 M $p66_{P243R}$/p51 and

HIV-1 O $p66_{P243R}$/p51 mutants; however the thermostabilities of these enzymes were similar to wild-type HIV-1 M p66/p51 and HIV-1 O p66/p51 (unpublished results). This finding suggests that this stabilization strategy is not applicable to HIV-1 RT. However, another possibility remains that Pro243 of HIV-1 RT does not correspond to Glu286 of MMLV RT.

For MMLV RT, unlike HIV-1 RT, the structure of the RNase H domain was determined from a crystal of the isolated RNase H domain of MMLV RT (Ile498–Leu671) (Lim et al. 2006), but not from a crystal of the full length MMLV RT (Thr24–Leu671) (Das and Georgiadis, 2004). For xenotropic murine leukemia virus-related virus (XMRV) RT, which differs only at five amino acid residues from MMLV RT, the structure of the RNase H domain was determined from a crystal of the isolated RNase H domain (Kim et al. 2012), but not from a crystal of the full-length XMRV RT (Nowak et al. 2013). Therefore, it remains unknown how the RNase H domain is positioned in an intact molecule. For HIV-1 RT, the RNase H domain of p66 is positioned far from the fingers, palm, and thumb subdomains of p66, but close to the connection subdomain of p66 and the thumb subdomain of p51 (Huang et al. 1988; Coté and Ruth, 2008). It has been reported that chimeric HIV-1 RT, which comprises p66 of HIV-1 M and p51 of HIV-1 O is more stable than a heterodimer containing p66 of HIV-1 O and p51 of HIV-1 M (Menéndez-Arias et al. 2001). In this study, the stability of p66/p51 was higher than that of $(p66)_2$ and $(p51)_2$ for HIV-1 O RT while they were similar for HIV-1 M RT (Fig. 5). Based on these findings, we speculate that the Asp443→Ala mutation alters the stability of HIV-1 RT by altering the structure of the RNase H domain and its interaction with the thumb subdomain of p51.

For HIV-1 M RT and HIV-1 O RT, Asp443 and Asp498 are important for RNase H

activity. In a previous study of HIV-1 M p66/p51, the Asp443→Ala mutation did not alter stability (Mizrahi et al. 1994), whereas the Asp443→Asn mutation decreased it (Mizrahi et al. 1994) and the Asp498→Asn mutation increased it (DeStefano et al. 1994). The reason for the discrepancy regarding the stabilizing effects of the Asp443→Ala mutation observed in this study and a previous report (Mizrahi et al. 1994) is unknown. One possibility is that in this study, p51 and p66 were separately expressed in the soluble fractions and then mixed, whereas in the previous study, the p66 precursor and the virus-encoded protease were co-expressed in the soluble fraction, allowing the viral protease to cleave the p66 precursor into p66 and p51 (Mizrahi et al. 1989; 1994). We propose that the mutation in the RNase H domain affects proteolytic processing of the p66 precursor, as the authors in that study of a previous study noted (Mizrahi et al. 1994).

In this study, the effects of the Asp443→Ala mutation on HIV-1 M RT and HIV-1 O RT were characterized. HIV-1 O $p66_{D443A}$/p51 is more stable than HIV-1 M $p66_{D443A}$/p51. It has been reported that HIV-1 M RT and HIV-1 O RT have higher affinity for substrates and are less susceptible to formamide (Konishi et al. 2013). It has also been reported that the Lys65→Arg, Arg78→Ala, Val75→Ile, Asp443→Asn, and Glu478→Gln mutations increased the fidelity of HIV-1 O RT (Barrioluengo et al. 2011; Álvarez et al. 2013). Taken together, these data suggest that the use of multiple HIV-1 O RT variants designed to have even higher stability and fidelity might be the most attractive for practical use in cDNA synthesis in the future.

Acknowledgments

This study was supported in part (K.Y.) by Grants-in-Aid for Scientific Research (nos. 19580104 and 21580110) from the Japan Society for the Promotion of Science and the Towa foundation for food research.

References

Álvarez M, Barrioluengo V, Afonso-Lehmann RN, Menéndez-Arias L (2013) Altered error specificity of RNase H-deficient HIV-1 reverse transcriptases during DNA-dependent DNA synthesis. Nucleic Acid Res 41:4601–4612

Álvarez M, Matamoros T, Menéndez-Arias L (2009) Increased thermostability and fidelity of DNA synthesis of wild-type and mutant HIV-1 group O reverse transcriptases. J Mol Biol 392:872–884

Arezi B, Hogrefe H (2009) Novel mutations in Moloney murine leukemia virus reverse transcriptase increase thermostability through tighter binding to template-primer. Nucleic Acids Res 37:473–481

Baranauskas A, Paliksa S, Alzbutas G, Vaitkevicius M, Lubiene J, Letukiene V, Burinskas S, Sasnauskas G, Skirgaila R (2012) Generation and characterization of new highly thermostable and processive M-MuLV reverse transcriptase variants. Protein Eng Des & Sel 25:657–668

Barrioluengo V, Álvarez M, Barbieri D, Menéndez-Arias L (2011) Thermostable HIV-1 group O reverse transcriptase variants with the same fidelity as murine leukaemia virus reverse transcritpase. Biochem J 436:599–607

Bavand MR, Wagner R, Richmond TJ (1993) HIV-1 reverse transcriptase: polymerization properties of the p51 homodimer compared to the p66/p51

heterodimer. Biochemistry 32:10543–10552

Bradford MM (1976) A rapid and sensitive method for the quantitation of microgram quantities of protein utilizing the principle of protein-dye binding. Anal Biochem 72:248−254

Buonaguro L, Tornesello ML, Buonaguro FM (2007) Human immunodeficiency virus type 1 subtype distribution in the worldwide epidemic: pathogenetic and therapeutic implications. J Virol 81:10209–10219

Coté ML, Roth MJ (2008) Murine leukemia virus reverse transcriptase: structural comparison with HIV-1 reverse transcriptase. Virus Res 134:186–202

DeStefano JJ, Wu W, Seehra J, McCoy J, Laston D, Albone E, Fay PJ, Bambara RA (1994) Characterization of an RNase H deficient mutant of human immunodeficiency virus-1 reverse transcriptase having an aspartate to asparagine change at position 498. Biochim Biophys Acta 1219:380–388

Das D, Georgiadis MM (2004) The crystal structure of the monomeric reverse transcriptase from Moloney murine leukemia virus. Structure 12:819–829

di Marzo Veronese F, Copeland TD, DeVico AL, Rahman R, Oroszlan S, Gallo RC, Sarngadharan MG (1986) Characterization of highly immunogenic p66/p51 as the reverse transcriptase of HTLV-III/LAV. Science, 231:1289–1291

Ding J, Das K, Hsiou Y, Sarafianos SG, Clark AD Jr, Jacobo-Molina A, Tantillo C, Hughes SH, Arnold E (1998) Structure and functional implications of the polymerase active site region in a complex of HIV-1 RT with a double-stranded DNA template-primer and an antibody Fab fragment at 2.8 Å resolution. J Mol Biol 284:1095–1111

Gerard GF, Potter RJ, Smith MD, Rosenthal K, Dhariwal G, Lee J, Chatterjee DK

(2002) The role of template-primer in protection of reverse transcriptase from thermal inactivation. Nucleic Acids Res 30:3118–3129

Huang H, Chopra R, Verdine GL, Harrison SC (1998) Structure of covalently trapped catalytic complex of HIV-1 reverse transcriptase: implications for drug resistance. Science 282:1669–1675

Hostomsky Z, Hostomska Z, Fu TB, Taylor J (1992) Reverse transcriptase to human immunodeficiency virus type 1: functionality of subunits of the heterodimer in DNA synthesis. J Virol 66:3179–3182

Kim JH, Kang S, Jung SK, Yu KR, Chung SJ, Chung BH, Erikson RL, Kim BY, Kim SJ (2012) Crystal structure of xenotropic murine leukaemia virus-related virus (XMRV) ribonulcease H. Biosci Rep 32:455–463

Kimmel AR, Berger SL (1987) Preparation of cDNA and the generation of cDNA libraries: overview. Methods Enzymol 152:307–316

Kotewicz ML, D'Alessio JM, Driftmier KM, Blodgett KP, Gerard GF (1985) Cloning and overexpression of Moloney murine leukemia virus reverse transcriptase in *Escherichia coli*. Gene 35:249–258.

Konishi A, Yasukawa K, Inouye K (2012) Improving the thermal stability of avian myeloblastosis virus reverse transcriptase α subunit by site-directed mutagenesis. Biotechnol Lett 34:1209–1215

Konishi A, Shinomura M, Yasukawa K (2013) Enzymatic characterization of human immunodeficiency virus type 1 reverse transcriptase for use in cDNA synthesis. Appl Biochem Biotechnol 169:77−87

Le Grice SF, Naas T, Wohlgensinger B, Schatz O (1991) Subunit-selective mutagenesis indicates minimal polymerase activity in heterodimer-associated p51 HIV-1

reverse transcriptase. EMBO J 10:3905–3911

Lim D, Gregorio GG, Bingman C, Martinez-Hackert E, Hendrickson WA, Goff SP (2006) Crystal structure of the Moloney murine leukemia virus RNaseH domain. J Virol 80: 8379–8389

Marko RA, Liu HW, Ablenas CJ, Ehteshami M, Götte M, Cosa G (2013) Binding kinetics and affinities of heterodimeric versus homodimeric HIV-1 reverse transcriptase on DNA-DNA substrate at the single-molecular level. J Phys Chem B 117: 4560–4567

Menéndez-Arias L, Abraha A, Quiñones-Mateu ME, Mas A, Camarasa MJ, Arts EJ (2001) Functional chatacterization of chimeric reverse transcriptases with polypeptide subunits of highly divergent HIV-1 group M and O strains. J Biol Chem 276:27470–27479

Mizrahi V, Brooksbank RL, Nkabinde NC (1994) Mutagenesis of the conserved aspartic acid 443, glutamic acid 478, asparagine 494, and aspartic acid 498 residues in the ribonuclease H domain of p66/p51 human immunodeficiency virus type 1 reverse transcriptase. J Biol Chem 269:19245–19249

Mizrahi V, Lazarus GM, Miles LY, Meyers CA, Debouck C (1989) Recombinant HIV-1 reverse transcriptase: purification, primary structure, and polymerase/ribonuclease H activities. Arch Biochem Biophys 273:347–358

Mizuno M, Yasukawa K, Inouye K (2010) Insight into the mechanism of the stabilization of Moloney murine leukaemia virus reverse transcriptase by eliminating RNase H activity. Biosci Biotechnol Biochem 74:440–442

Nowak W, Potrzebowski W, Konarev PV, Rausch JW, Bona MK, Svergun DI, Bujnicki JM, Le Grice SFJ, Nowotny M (2013) Structural analysis of monomeric retroviral

reverse transcriptase in complex with an RNA/DNA hybrid. Nucleic Acids Res 41:3874–3887

Patel PH, Jacobo-Molina A, Ding J, Tantillo C, Clark AD Jr, Raag R, Nanni RG, Hughes SH, Arnold E (1995) Insights into DNA polymerization mechanisms from structure and function analysis of HIV-1 reverse transcriptase. Biochemistry 34:5351–5363

Quiňones-Mateu ME, Soriano V, Domingo E, Menéndez-Arias L (1997) Characterization of the reverse transcriptase of a human immunodeficiency virus type 1 group O isolate. Virology 236:364–373

Venezia CF, Meany BJ, Braz VA, Barkley MD (2009) Kinetics of association and dissociation of HIV-1 reverse transcriptase. Biochemistry 48:9084–9093

Yasukawa K, Agata N, Inouye K (2010a) Detection of *cesA* mRNA from *Bacillus cereus* by RNA-specific amplification. Enzyme Microb Technol 46:391−396

Yasukawa K, Mizuno M, Konishi A, Inouye K (2010b) Increase in thermal stability of Moloney murine leukaemia virus reverse transcriptase by site-directed mutagenesis. J Biotechnol 150:299–306

Yasukawa K, Mizuno M, Inouye K (2009) Characterization of Moloney murine leukaemia virus/avian myeloblastosis virus chimeric reverse transcriptases J Biochem 145:315-324

Yasukawa K, Nemoto D, Inouye K (2008) Comparison of the thermal stabilities of reverse transcriptases from avian myeloblastosis virus and Moloney murine leukaemia virus. J Biochem 143:261–268

Table 1

Kinetic parameters of RT in the to incorporation of dTTP into poly(rA)-p$(dT)_{15}$ (T/P) at 37ºC.

RT	$K_{m,\ dTTP}$ (μM)	$K_{m,T/P}$ (μM)	k_{cat} (s^{-1})
HIV-1 M $(p51)_2$	34 ± 9	2.1 ± 0.8	0.19 ± 0.02
HIV-1 M $(p66)_2$	16 ± 3	1.6 ± 0.5	0.19 ± 0.01
HIV-1 M RT p66/p51	18 ± 5	0.75 ± 0.30	0.60 ± 0.03
HIV-1 O $(p51)_2$	130 ± 50	3.5 ± 1.0	0.73 ± 0.14
HIV-1 O $(p66)_2$	44 ± 5	1.3 ± 0.2	2.1 ± 0.1
HIV-1 O RT p66/p51	23 ± 3	1.7 ± 0.2	3.3 ± 0.1

Average of triplicate determinations with SD value is shown.

Figure legends

Fig. 1. Expression plasmids. The structures of pET-HisHIVMp66, pET-HisHIVMp51, pET-HisHIVOp66, and pET-HisHIVOp51 are shown. The asterisk indicates the termination codon.

Fig. 2. SDS-PAGE under reducing conditions. Coomassie Brilliant Blue-stained 10% SDS-polyacrylamide gel is shown. (A) HIV-1 M RT. (B) HIV-1 O RT.

Fig. 3. Dependence on substrate concentration of the reaction rate (v_o) in HIV-1 RT catalyzed incorporation of dTTP into poly(rA)-p(dT)$_{15}$. Dependence on dTTP (A, C) and poly(rA)-p(dT)$_{15}$ (B, D) concentrations of HIV-1 M (A, B) and O (C, D) RT are shown. The initial concentrations of HIV-1 M $(p51)_2$, $(p66)_2$ and p66/p51 were 100, 100, and 20 nM, respectively, and those of HIV-1 O $(p51)_2$, $(p66)_2$ and p66/p51 were 40, 8, and 8 nM, respectively. The initial concentration of poly(rA)-p(dT)$_{15}$ was 25 μM (A, C), and that of dTTP was 200 μM (B, D). Solid lines represent the best fit of the Michaelis-Menten equation with the non-linear least squares method. Symbols for the enzymes: $(p51)_2$ (open circle), $(p66)_2$ (open triangle), and p66/p51 (open square).

Fig. 4. Dependence on enzyme concentration of HIV-1 RT-catalyzed cDNA synthesis. cDNA synthesis was carried out with various concentrations of $(p51)_2$, $(p66)_2$, and p66/p51 at 46°C. Then, PCR was carried out. Marker DNAs and the amplified products were separated on 1.0% agarose gels and stained with ethidium bromide. Lane M, DNA marker. RT concentration in cDNA synthesis: 0 (lane 1), 1×10^{-6} (lane 2), 1×10^{-5} (lane

3), 1×10^{-4} (lane 4), 1×10^{-3} (lane 5), 1×10^{-2} (lane 6), 0.1 (lane 7), 1 (lane 8), 10 (lane 9), and 100 nM (lane 10). The arrow indicates the expected size (601 bp) of the amplified products.

Fig. 5. Irreversible thermal inactivation of HIV-1 RT. HIV-1 M RT $(p51)_2$, $(p66)_2$, p66/p51, and $p66_{D443A}$/p51 (250, 50, 20, and 20 nM, respectively) or HIV-1 O $(p51)_2$, $(p66)_2$, p66/p51, and $p66_{D443A}$/p51 (100, 20, 20, and 20 nM, respectively) was incubated at 42−56°C in the presence of poly(rA)-$p(dT)_{15}$ (T/P) (28 μM) for 10 min. Then, the reaction to incorporate dTTP into poly(rA)-$p(dT)_{15}$ was carried out at 37°C. The relative activity of HIV-1 RT was defined as the ratio of the initial reaction rate with incubation for 10 min to that without incubation.

Fig. 6. Dependence on reaction temperature of HIV-1 RT-catalyzed cDNA synthesis. cDNA synthesis was carried out with 1 nM HIV-1 M p66/p51, HIV-1 M $p66_{D443A}$/p51, HIV-1 O p66/p51, or HIV-1 O $p66_{D443A}$/p51 at 46−68°C. Then, PCR was carried out. Marker DNAs and amplified products were separated on 1.0% agarose gels and stained with ethidium bromide.

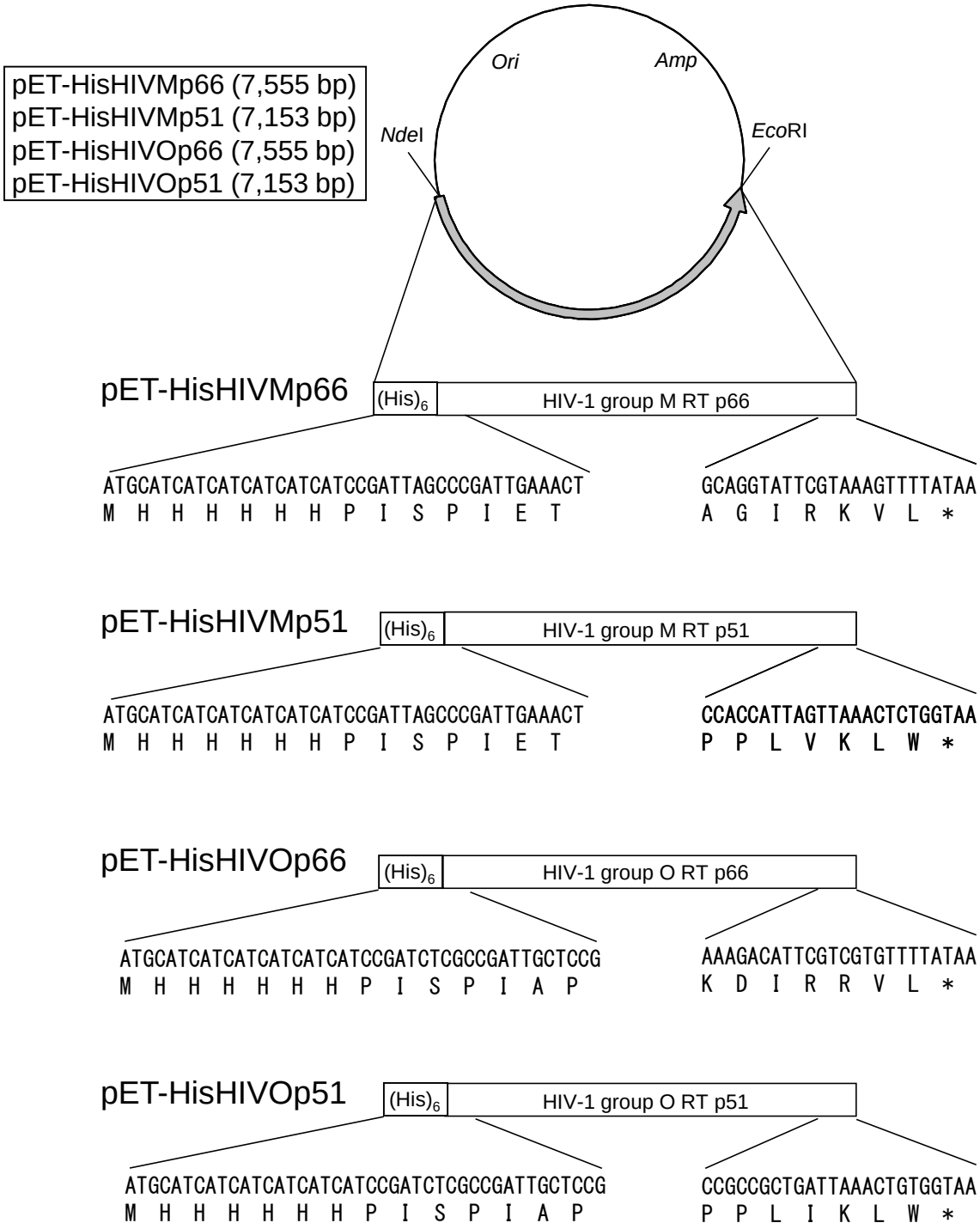
pET-HisHIVMp66 (7,555 bp)
pET-HisHIVMp51 (7,153 bp)
pET-HisHIVOp66 (7,555 bp)
pET-HisHIVOp51 (7,153 bp)
Ori
Amp
NdeI
EcoRI
pET-HisHIVMp66
(His)6
HIV-1 group M RT p66
ATGCATCATCATCATCATCATCCGATTAGCCCGATTGAAACT
M H H H H H H P I S P I E T
GCAGGTATTCGTAAAGTTTTATAA
A G I R K V L *
pET-HisHIVMp51
(His)6
HIV-1 group M RT p51
ATGCATCATCATCATCATCATCCGATTAGCCCGATTGAAACT
M H H H H H H P I S P I E T
CCACCATTAGTTAAACTCTGGTAA
P P L V K L W *
pET-HisHIVOp66
(His)6
HIV-1 group O RT p66
ATGCATCATCATCATCATCATCCGATCTCGCCGATTGCTCCG
M H H H H H H P I S P I A P
AAAGACATTCGTCGTGTTTTATAA
K D I R R V L *
pET-HisHIVOp51
(His)6
HIV-1 group O RT p51
ATGCATCATCATCATCATCATCCGATCTCGCCGATTGCTCCG
M H H H H H H P I S P I A P
CCGCCGCTGATTAAACTGTGGTAA
P P L I K L W *

Fig. 1

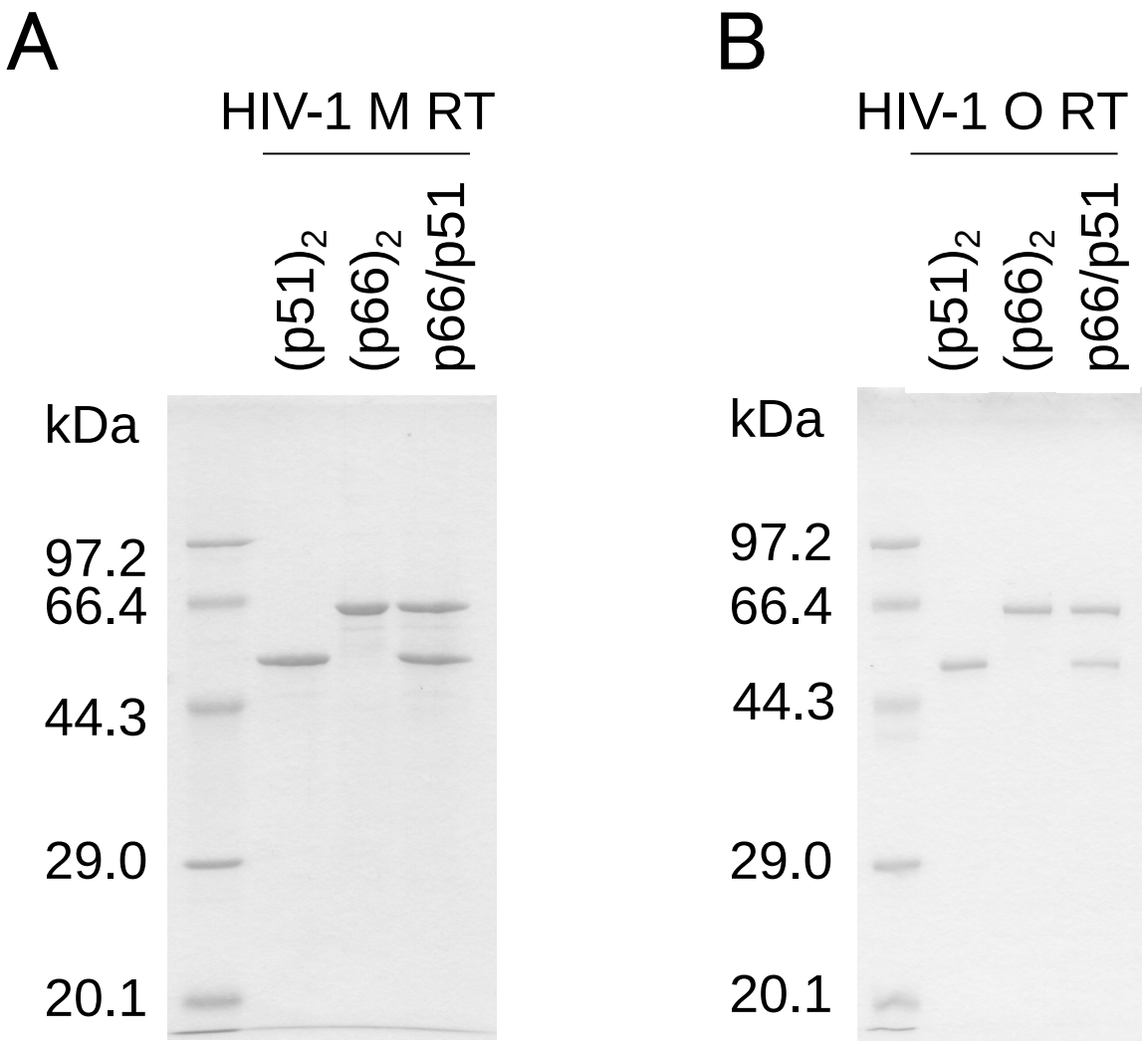
A
HIV-1 M RT
(p51)2
(p66)2
p66/p51
kDa
97.2
66.4
44.3
29.0
20.1
B
HIV-1 O RT
(p51)2
(p66)2
p66/p51
kDa
97.2
66.4
44.3
29.0
20.1

Fig. 2

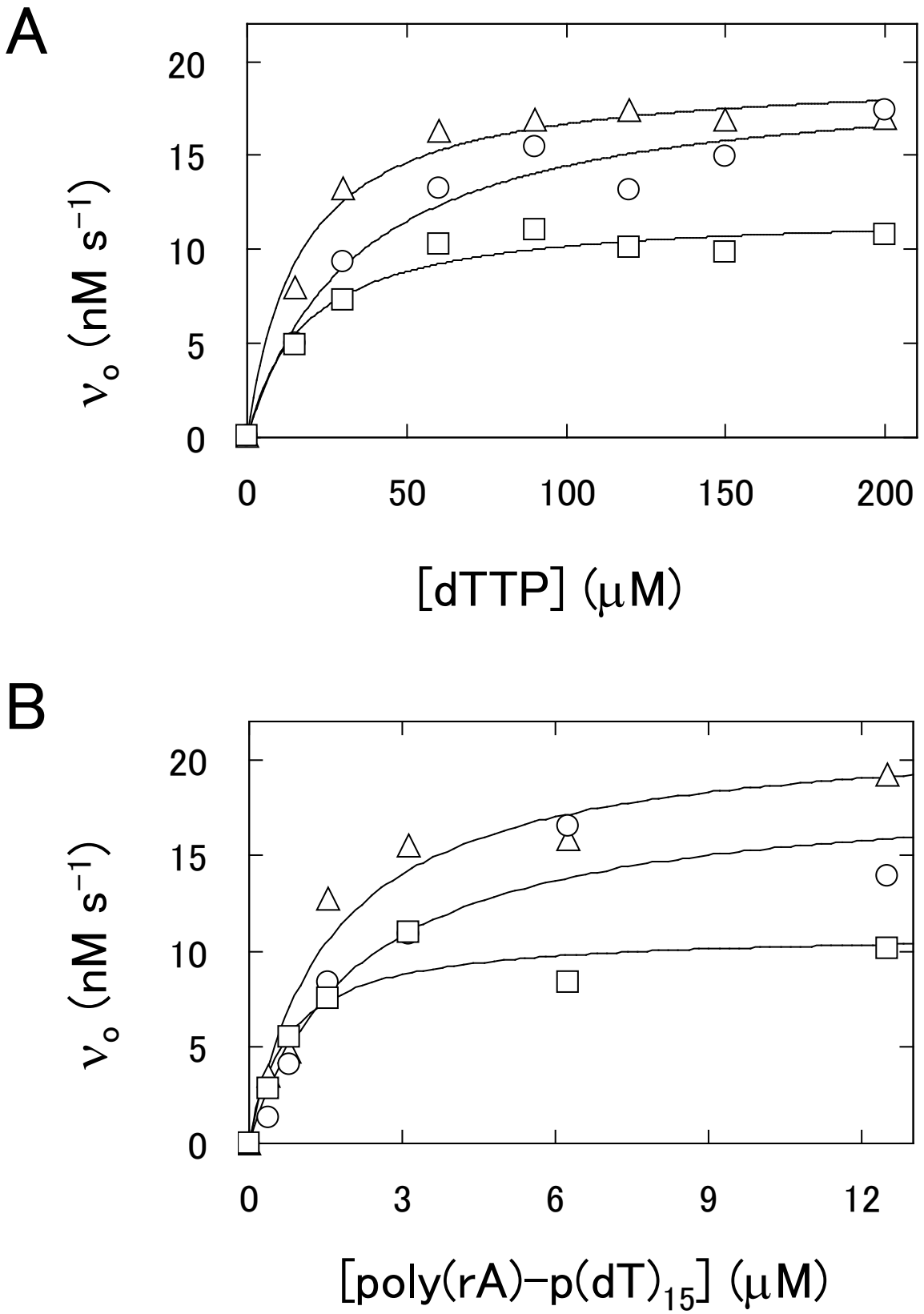
A
20
15
10
5
0
v_o (nM s^{-1})
0
50
100
150
200
[dTTP] (μM)
B
20
15
10
5
0
v_o (nM s^{-1})
0
3
6
9
12
[poly(rA)–p(dT)$_{15}$] (μM)

Fig. 3

C

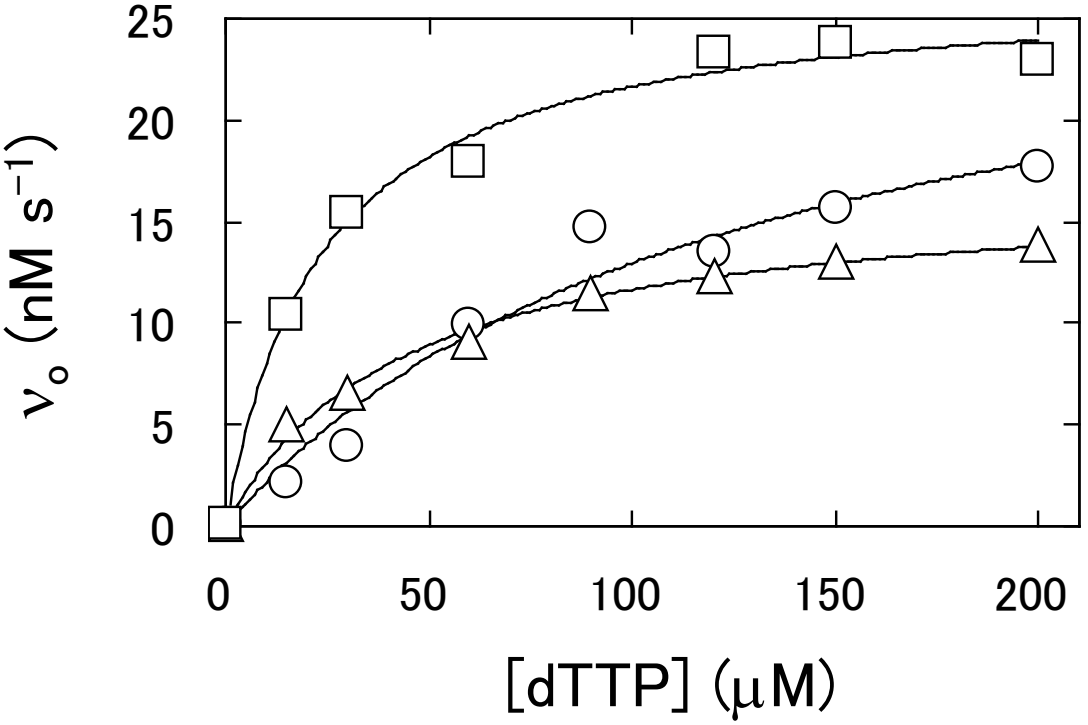
25
20
15
10
5
0
v_o (nM s^{-1})
0
50
100
150
200
[dTTP] (μM)

D

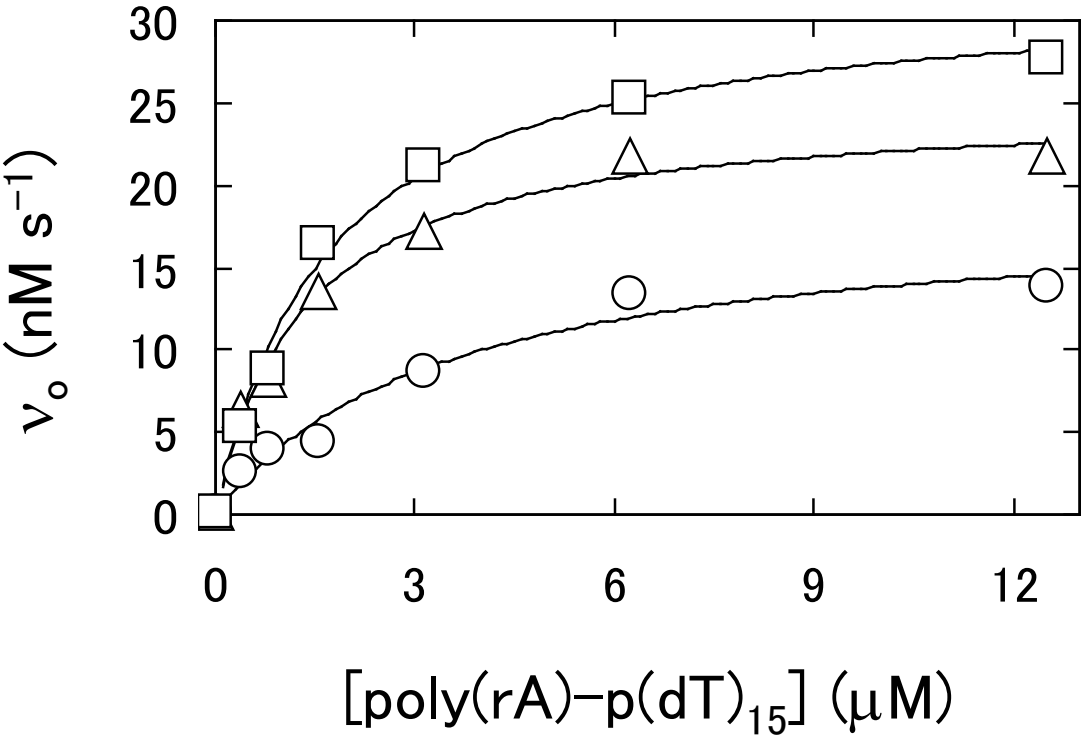
30
25
20
15
10
5
0
v_o (nM s^{-1})
0
3
6
9
12
[poly(rA)–p(dT)$_{15}$] (μM)

Fig. 3

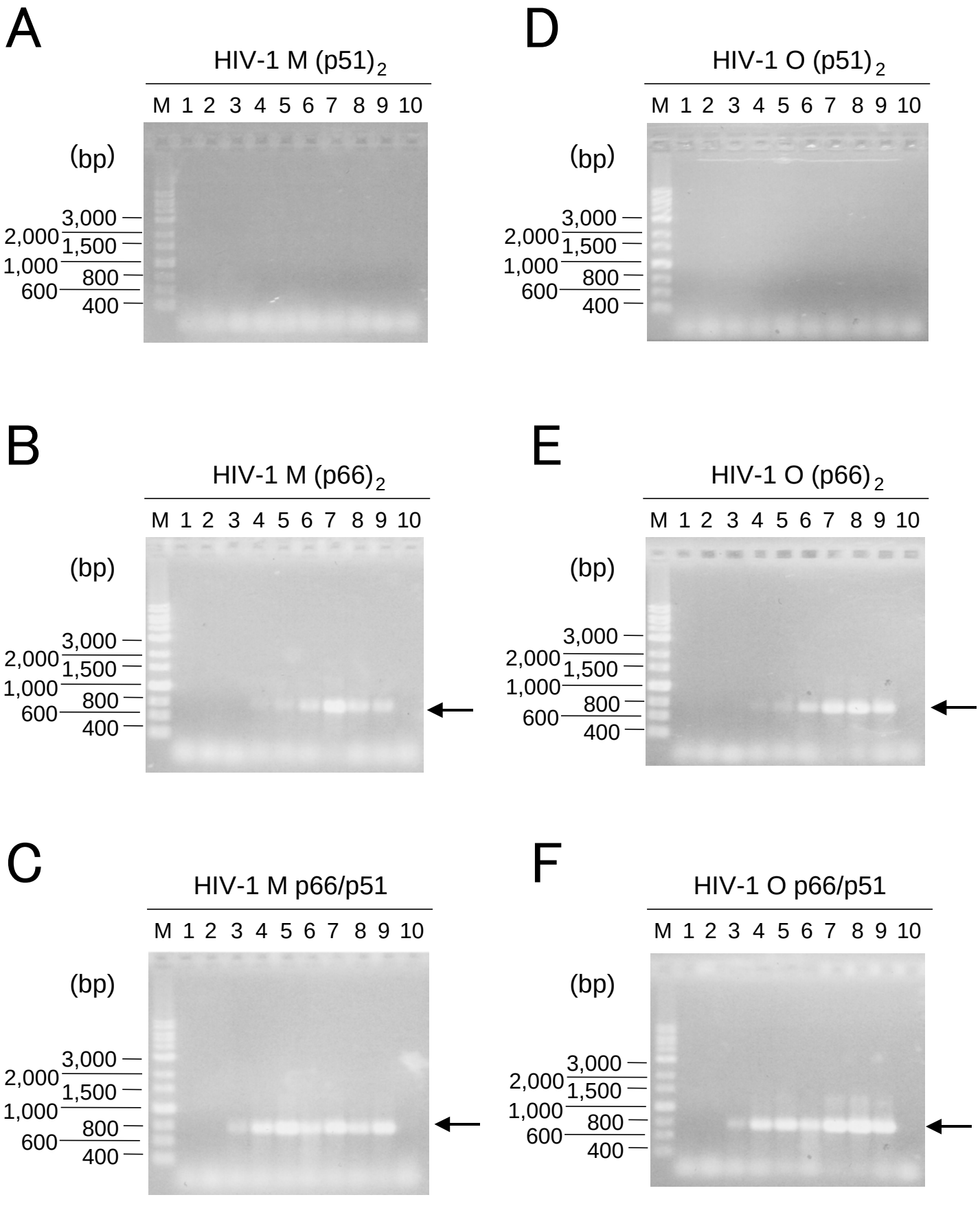
A
HIV-1 M (p51)2
M 1 2 3 4 5 6 7 8 9 10
(bp)
3,000
2,000
1,500
1,000
800
600
400
D
HIV-1 O (p51)2
M 1 2 3 4 5 6 7 8 9 10
(bp)
3,000
2,000
1,500
1,000
800
600
400
B
HIV-1 M (p66)2
M 1 2 3 4 5 6 7 8 9 10
(bp)
3,000
2,000
1,500
1,000
800
600
400
E
HIV-1 O (p66)2
M 1 2 3 4 5 6 7 8 9 10
(bp)
3,000
2,000
1,500
1,000
800
600
400
C
HIV-1 M p66/p51
M 1 2 3 4 5 6 7 8 9 10
(bp)
3,000
2,000
1,500
1,000
800
600
400
F
HIV-1 O p66/p51
M 1 2 3 4 5 6 7 8 9 10
(bp)
3,000
2,000
1,500
1,000
800
600
400

Fig. 4

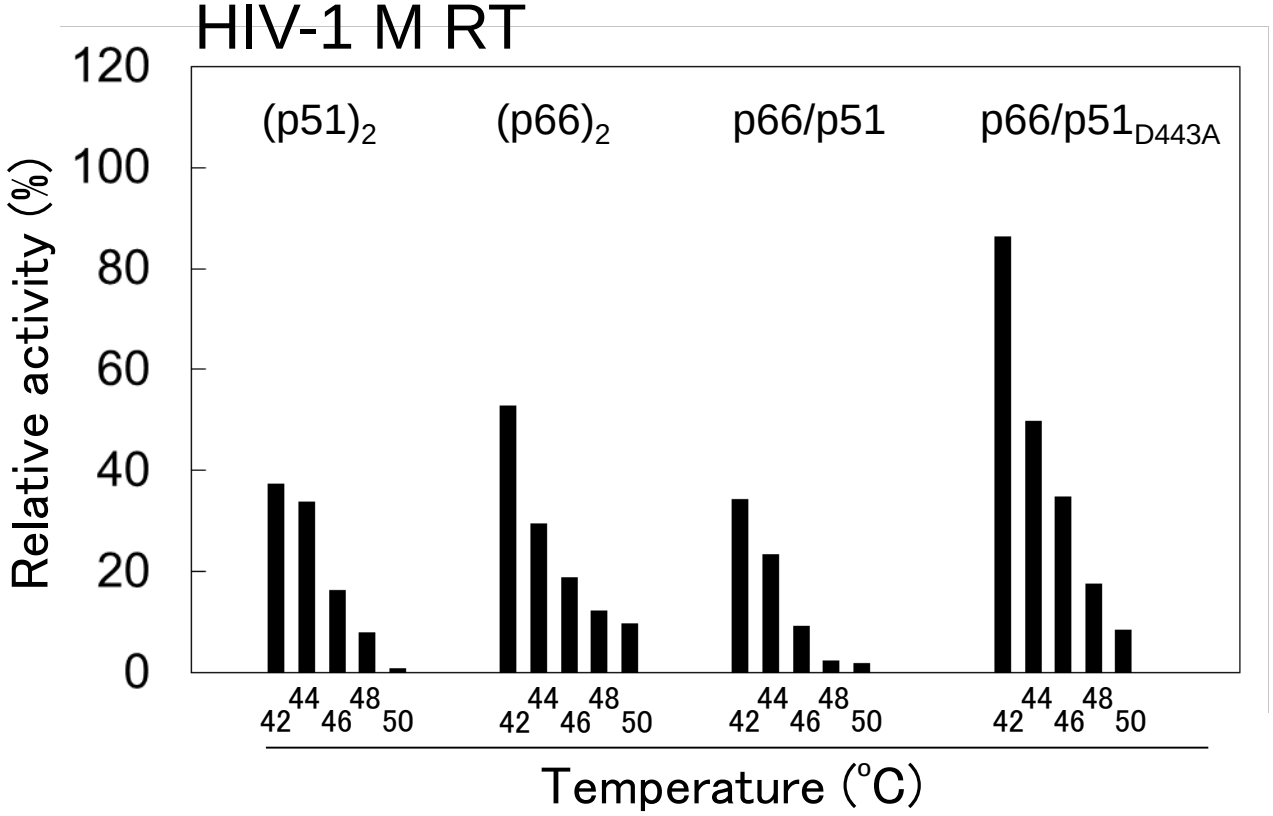
HIV-1 M RT
(p51)2
(p66)2
p66/p51
p66/p51D443A
Relative activity (%)
120
100
80
60
40
20
0
42 44 46 48 50
Temperature (°C)

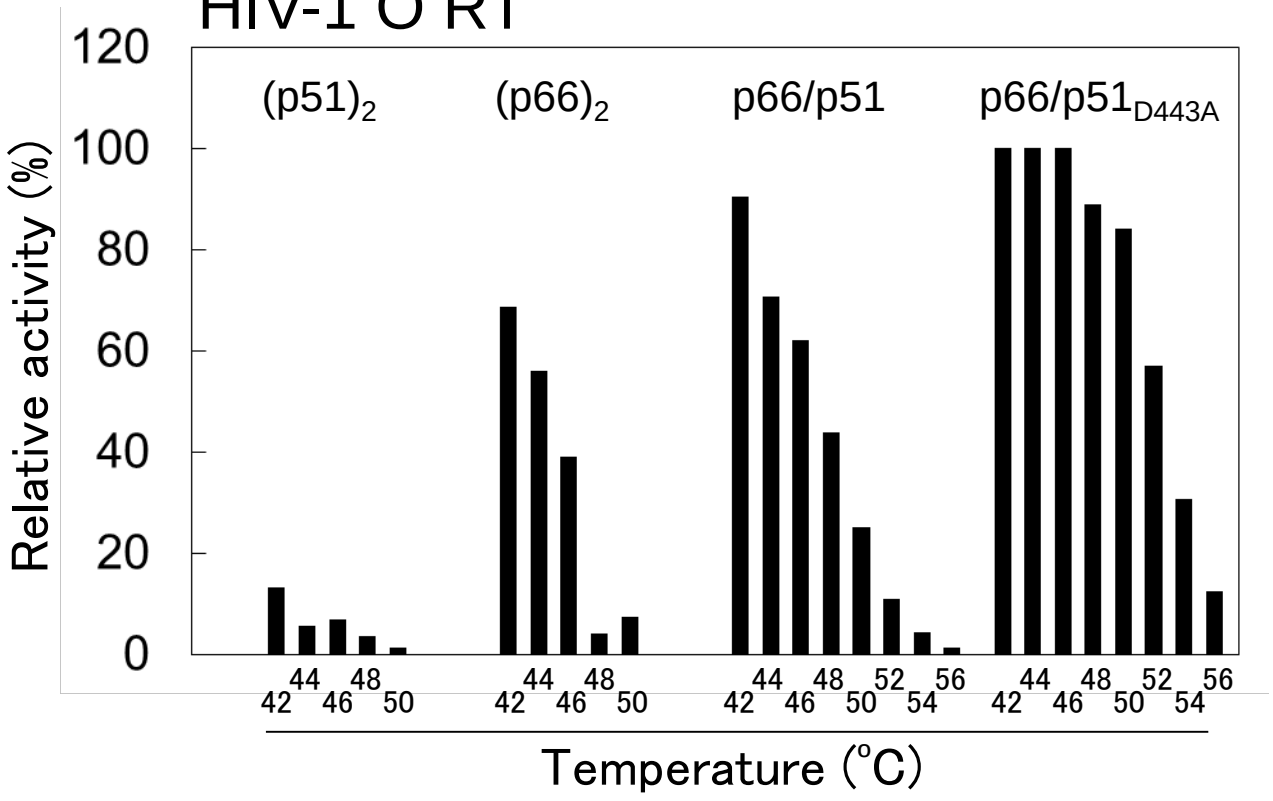
HIV-1 O RT
(p51)2
(p66)2
p66/p51
p66/p51D443A
Relative activity (%)
120
100
80
60
40
20
0
42 44 46 48 50
42 44 46 48 50
42 44 46 48 50 52 54 56
42 44 46 48 50 52 54 56
Temperature (°C)

Fig. 5

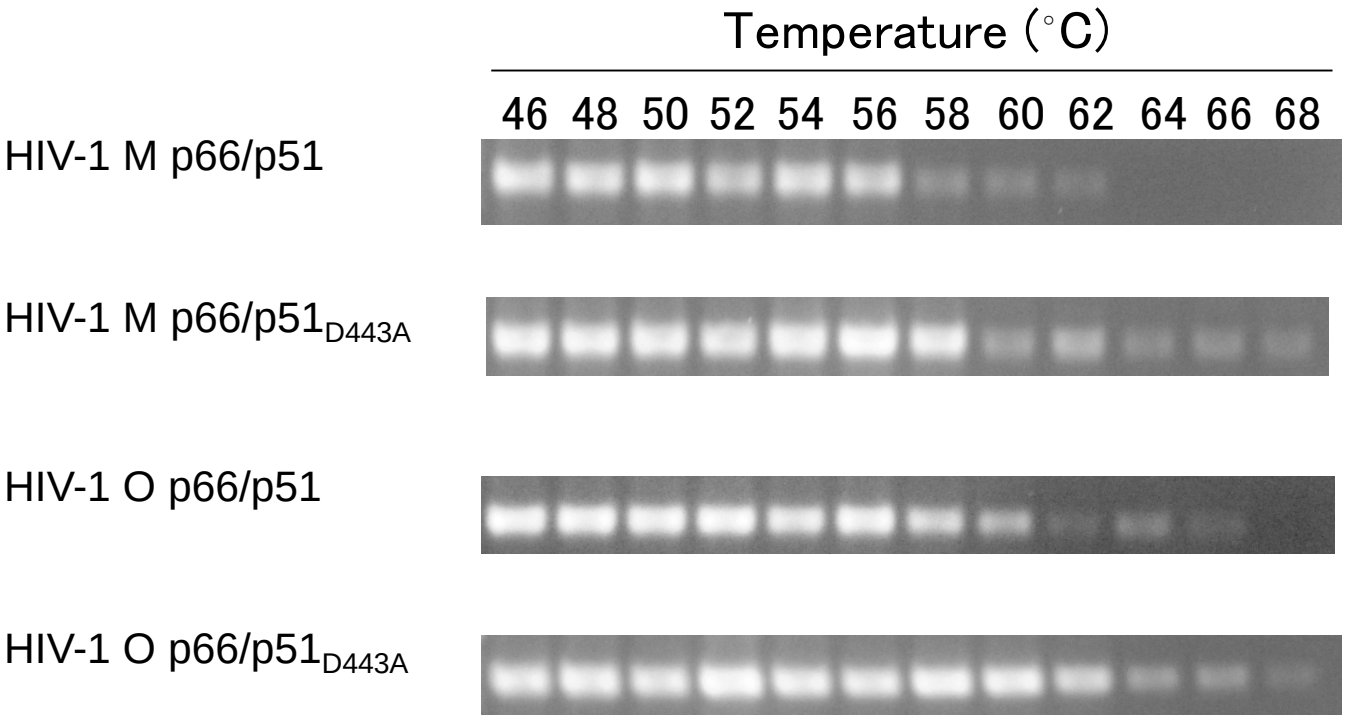
Temperature (°C)
46 48 50 52 54 56 58 60 62 64 66 68
HIV-1 M p66/p51
HIV-1 M p66/p51D443A
HIV-1 O p66/p51
HIV-1 O p66/p51D443A

Fig. 6